

## STUDIES OF HOT B SUBDWARFS. V. CONTINUING INVESTIGATION OF THE C, N, AND Si ABUNDANCE PATTERNS IN THE ATMOSPHERES OF sdB STARS

R. LAMONTAGNE,<sup>1</sup> F. WESEMAEL,<sup>1,2</sup> AND G. FONTAINE<sup>1,2,3</sup>

Département de Physique, Université de Montréal  
 Received 1986 October 16; accepted 1986 December 19

### ABSTRACT

High-dispersion ultraviolet observations of two hot, hydrogen-rich subdwarfs have been obtained with the *IUE* observatory, and are presented. These data are analyzed with model atmosphere techniques, and element abundances for C, N, and Si are derived. Both PG 0342+026 ( $T_e = 21,800$  K) and PG 1104+243 ( $T_e = 27,200$  K) display abundances of these ions consistent with trends observed previously in generally hotter sdB and sdOB stars. In particular, the strong silicon underabundance observed in those is also seen in PG 1104+243. These results provide additional constraints on current models invoking element diffusion—with or without competing particle transport processes—as the source of the abundance peculiarities observed in hot, hydrogen-rich subdwarfs.

*Subject headings:* stars: abundances — stars: atmospheres — stars: early-type — stars: subdwarfs — ultraviolet: spectra

### I. INTRODUCTION

A vastly improved knowledge of the abundance patterns in hot, evolved stars stands among the many successes of the *International Ultraviolet Explorer* (*IUE*) observatory (e.g., Vauclair and Liebert 1987). Indeed, the largest fraction of what is known today about the abundances of heavy elements in the photospheres of hot white dwarfs and subdwarfs originates with the *IUE*. In the case of the hot hydrogen-rich subdwarfs, this is perhaps most evident in a comparison of the results summarized in Greenstein and Sargent (1974) with recent analyses of *IUE* observations of the very brightest B and OB subdwarfs (Baschek *et al.* 1982, hereafter BKSS; Baschek, Höflich, and Scholz 1982, hereafter BHS). While the former review reports only a few metal lines in high-dispersion optical work, the latter papers discuss the presence of more than 1500 metal lines—a large fraction of which remain unidentified—in the ultraviolet spectra of HD 149382 and Feige 66, two hot hydrogen-rich subdwarfs. Clearly, the *IUE* provides a unique opportunity of identifying and understanding the patterns of heavy-element abundances in hot subdwarf stars.

In a previous paper (Lamontagne *et al.* 1985, hereafter Paper I), we presented the first results of such a program: high-dispersion *IUE* observations were presented for three hydrogen-rich hot subdwarfs ( $V \approx 11.4$ –12), and model atmosphere analyses of the C, N, and Si line spectrum were performed. While BKSS and BHS had extended their analyses to many more elements in their two bright targets, the relative faintness of more typical B and OB subdwarfs (by current *IUE* high-dispersion standards) precludes the investigation of anything but the most abundant or intrinsically important elements.

The fundamental result of Paper I was, we believe, the identification of definite trends in element abundance patterns in hydrogen-rich subdwarfs: the observed carbon abundance seemed to decrease with increasing  $T_e$ ; nitrogen appeared in nearly solar abundances over the whole temperature range; lastly, silicon appeared to be in solar abundance below 30,000 K, but strikingly underabundant (by more than 5 dex) at higher temperatures.

Continuing studies of this kind are essential to our understanding of the nature of B subdwarfs, since they provide an observational testing ground for the idea that diffusion processes, including radiative element support, might be dominant in determining the metal abundance at the photosphere of subdwarf stars (BKSS; BHS; Heber *et al.* 1984*a, b*; Paper I; Michaud *et al.* 1985). Accordingly, we present here abundance analyses of two additional hydrogen-rich subdwarfs selected from the Palomar-Green survey (Green, Schmidt, and Liebert 1986): PG 1104+243 ( $y = 11.26$ ) and PG 0342+026 ( $y = 10.96$ ). The former is described as binary in the PG survey. This is confirmed by our subsequent *BVRI* photometry (Allard *et al.* 1987*a*) and optical spectrophotometry of the system. Ferguson, Green, and Liebert (1984) have recently deconvolved the energy distribution of the system and derive a spectral type K2 for the secondary. Both subdwarfs fit nicely in temperature domains not covered in previous studies of this kind (see Fig. 6 of Paper I): PG 0342+026 is a cool sdB star below 25,000 K, while PG 1104+243 fits in the gap between 26,000 K and 32,000 K, where no object has yet been analyzed.

In § II of this paper, we describe in detail the observational data used for our analysis. In addition to the high-dispersion ultraviolet spectra used in the abundance determinations, we also make use of lower dispersion spectrophotometry and optical photometry to fix the stellar parameters. Those are determined in § III, and the metal abundance results are given in § IV. We provide, in § V, an updated view of the abundance patterns of heavy elements in hydrogen-rich subdwarfs, and discuss the implication of these additional results for our knowledge of diffusion processes in the envelopes and atmospheres of these objects.

<sup>1</sup> Visiting Astronomer, Kitt Peak National Observatory, National Optical Astronomy Observatories, which is operated by AURA, Inc., under contract with the National Science Foundation.

<sup>2</sup> Guest Observer with the *International Ultraviolet Explorer* satellite, which is sponsored and operated by the National Aeronautics and Space Administration, by the Science Research Council of the United Kingdom, and by the European Space Agency.

<sup>3</sup> E. W. R. Steacie Memorial Fellow.

## II. OBSERVATIONS AND DATA REDUCTION AND ANALYSIS

a) *IUE Data*

High-dispersion *IUE* spectra of our two program objects were obtained with the SWP camera in 1986. The wavelength range covered is 1100–2100 Å. The exposure level of both images is adequate and ranges from 95 to 110 DN above background.

In addition, these two objects were also observed in the low-dispersion mode with the SWP and LWP cameras, in order to construct ultraviolet energy distributions. All observations were carried out through the large (10" × 20") aperture. A complete log of *IUE* observations is given in Table 1. The late-type companion in PG 1104+243 is not expected to contribute any flux to the spectral region covered with the *IUE*.

b) *Optical Data*

Optical photometric and spectrophotometric observations were also carried out to complete the energy distribution of both stars and to determine the surface gravity of PG 0342+026. Both objects were observed within our extensive program of Strömgren photometry of hot (hydrogen-rich) subdwarf candidates. This program is being carried out with the 1.3 m reflector at the Kitt Peak National Observatory (KPNO), and additional details will be reported on in due course (Fontaine *et al.* 1987). In addition, we make use here of a spectrum of PG 0342+026 obtained 1984 August 11 with the IIDS system behind the Gold spectrograph attached to the KPNO 2.1 m reflector. The total integration time was 8 minutes. The 600 lines mm<sup>-1</sup> grating (No. 35) was used in second order and provided coverage of the 4050–5000 Å region. An entrance aperture of 6" was used, and the resulting spectral resolution was better than 4.25 Å. Although a spectrum of PG 1104+243 was also obtained in an earlier run with the same instrument configuration, no use of those data is made here since the spectrum of PG 1104+243 is contaminated by its cool companion and is thus not usable for surface gravity determination.

c) *Analysis of the High-Dispersion IUE Images*

ISM and photospheric radial velocities were obtained for both objects from measurements of velocity shifts of several appropriate lines. The ISM velocity was based, in part, on the line list given by Dean and Bruhweiler (1985, Table 3), and relies mostly on the identification of C I, N I, S II, and Si II lines. We measure  $v_{\text{ISM}} = +14 \pm 9 \text{ km s}^{-1}$  for PG 0342+026 and  $v_{\text{ISM}} = -19 \pm 10 \text{ km s}^{-1}$  for PG 1104+243. The determination of the photospheric radial velocities relies on the strongest among the C II, C III, and N III features. Typically ~12 lines or components are used for this measurement. We find  $v = +6 \pm 9 \text{ km s}^{-1}$  for PG 0342+026 and

$v = -18 \pm 6 \text{ km s}^{-1}$  for PG 1104+243. Of course, the similarity between photospheric and ISM radial velocities for each object precludes the separation of the blended ISM and photospheric components, and these remain hopelessly entangled. We note that no space velocity information is available in the PG catalog; the selection of the two particular stars observed in this program was thus based exclusively on consideration of effective temperature and apparent magnitude.

Our technique for the measurements of equivalent widths is unchanged from that discussed in detail in Paper I. In essence, we fit a spline through the desired region of each order, using visually selected collocation points, to determine a local continuum. The reliability of this method has been investigated in Paper I, and the reader is referred to that paper for additional details. Finally, the *IUE* background correction procedure based on the empirical work of Bruhweiler and Kondo (1982) is used throughout, as it was in Paper I. Our line identifications and width measurements are summarized in Table 2.

d) *Analysis of Low-Dispersion IUE Data*

One fundamental difference between previous work of Heber *et al.* (1984b), Heber (1986), Wesemael *et al.* (1985), and, to some extent, Paper I and the present work is the substitution of the LWP camera for the LWR camera used in earlier investigations. The LWP calibration used throughout this work is that of Cassatella and Harris (1983); for the SWP camera, the standard calibration of Bohlin and Holm (1980), augmented with the correction of Hackney, Hackney, and Kondo (1982), was used. The latest corrections to the zero-epoch absolute calibration of the SWP camera (Bohlin 1986) came to our attention after the completion of this analysis.

This switch in default long-wavelength camera is important for our analysis, since there might well be systematic differences in the calibrations of the LWP and LWR cameras (Imhoff 1983). Indeed, in one experiment, we calculated ratios in 40 Å bandpasses of LWR fluxes with LWP fluxes available for the hot hydrogen-rich subdwarf Feige 66 (LWR 3016, LWP 4883). The *average* spectral ratio obtained is LWR/LWP = 0.9; a wavelength dependence of that ratio is also clearly seen, with a broad minimum (at LWR/LWP ~ 0.85) present in the 2450–2700 Å range. No improvement is noted when appropriate sensitivity changes are applied to the fluxes from both cameras (Sonneborn 1984). We also note that the linearity errors for nonoptimum spectra discussed by Oliverson (1984) would, if anything, tend to make the observed LWR/LWP ratio larger than 1.

In an effort to reduce this complicated calibration problem to its simplest form, we have carried out some tests in which we scale the LWP fluxes by a *gray* empirical factor of 0.9. This is admittedly a crude, ad hoc procedure which glosses over all the minutiae of the calibration problems connected with the use of the current LWP intensity transfer function. However, we have found that this results in improved energy distribution fits in some, but not all, of the objects we have attempted to analyze (see Allard *et al.* 1987b). The effect of this correction for the fit to PG 0342+026 is discussed briefly in § IIIa.

## III. ATMOSPHERIC PARAMETERS AND METHOD OF ANALYSIS

a) *Atmospheric Parameters*

As was the case in Paper I, atmospheric parameters must first be determined for the two objects under analysis. This is done in standard fashion by fitting composite energy distribu-

TABLE 1  
*IUE* OBSERVATION LOG

Star	Image Sequence Number	Dispersion	$t_{\text{exp}}$
PG 1104+243.....	SWP 27465	High	210 <sup>m</sup>
	SWP 26173	Low	2 <sup>m</sup> 40 <sup>s</sup>
	LWP 6222	Low	4 <sup>m</sup>
PG 0342+026.....	SWP 27466	High	160 <sup>m</sup>
	SWP 27467	Low	1 <sup>m</sup> 50 <sup>s</sup>
	LWP 7462	Low	2 <sup>m</sup> 40 <sup>s</sup>

TABLE 2  
LINE IDENTIFICATIONS AND EQUIVALENT WIDTHS

ION	$\lambda_{\text{lab}}$	$E_i^a$ ( $\text{cm}^{-1}$ )	$W_\lambda(\text{m}\text{\AA})^b$	
			PG 0342+026	PG 1104+243
C II	1323.91/3.95	74932	173	88
	1334.53	0	R	356
	1335.66/5.71	64	223	171
C III	1175.7 <sup>c</sup>	52419	1248	904
	1247.38	102351	146	127
	1922.96/3.16	269961	177	103:
C IV	1548.19	0	159	265
	1550.77	0	183	273
N II	1886.82	149189	122:	55:
N III	1183.03	145876	125	103
	1184.54	145987	115	151
	1747.86	145876	73	180
	1751.24	145987	34	99
	1751.75	145987	49	206
	1804.31	245666	49	104:
	1805.5	245702	112	46:
N IV	1885.25	267242	89	76:
	1718.55	130695	<119 <sup>d</sup>	<145: <sup>d</sup>
N V	1238.82	0	<40	<40
	1242.80	0	<40	S
Si II	1190.42	0	129	136
	1193.29	0	191 <sup>e</sup>	365 <sup>e</sup>
	1194.50	287	189 <sup>f</sup>	88 <sup>f</sup>
	1197.39	287	80	83:
	1260.42	0	197	269
	1264.74	287	74	65:
	1265.00	287	79	...
	1304.37	0	125	147
	1309.28	287	110	99:
	1526.71	0	219	R
	1533.43	287	68	...
	Si III	1294.54	52984	259 <sup>g</sup>
1296.73		52984	170 <sup>h</sup>	198 <sup>h</sup>
1298.89/8.96		52984	262 <sup>i</sup>	61 <sup>i</sup>
1301.15		52984	134	72 <sup>d</sup>
1303.32		52985	131	...
1341.47/1.50		142945	166	...
1342.35/2.39/2.43		142945	152	...
1343.39		142945	110	...
1363.46/3.50		142945	87	N
1365.25/5.29		142945	R	N
Si IV	1393.76	0	363	<47
	1402.77	0	477	<81

<sup>a</sup> Excitation energy of lower level.

<sup>b</sup> "R" indicates a reseau mark, "S" a saturated pixel, ellipsis dots a feature missing or of doubtful identification, "N" a noisy spectral region, and a colon an uncertain measurement.

<sup>c</sup> Six components at 1174.93, 1175.26, 1175.59, 1175.71, 1175.99, 1176.36 Å.

<sup>d</sup> Unidentified blend ?

<sup>e</sup> Blend with C I  $\lambda\lambda$ 1193.264, 1193.393.

<sup>f</sup> Blend with C I  $\lambda\lambda$ 1194.488, 1194.615.

<sup>g</sup> Blend with Ti III  $\lambda$ 1294.69.

<sup>h</sup> Blend with N IV  $\lambda$ 1296.60, S IV  $\lambda$ 1296.61.

<sup>i</sup> Blend with Ti III  $\lambda$ 1298.97.

tions with fluxes predicted from model atmosphere calculations (e.g., Wesemael *et al.* 1985; Paper I; Allard *et al.* 1987b). The basic model grid is that of Kurucz (1979) which incorporated the heavy ultraviolet metal line blanketing often observed in B subdwarfs. Variable amounts of interstellar reddening are included in the fits. A comparison between results obtained with Kurucz's models and other grids can be found in Heber *et al.* (1984b) and Wesemael *et al.* (1985). The grid consists of models of fixed gravity and of solar abundance. The first assumption is quite adequate, since the energy distribution lacks gravity sensitivity in the subdwarf range of  $\log g = 5-6$ ; the second is more delicate since hydrogen-rich subdwarfs have, in general, nonsolar abundances of heavy elements (see the data summarized in Paper I). Clearly, the energy

distributions fits could probably be somewhat improved by using models of varying metal abundance. However, this is likely to be a rather complex (if not costly) enterprise, since the abundance with respect to solar values varies from element to element! At this stage, theoretical energy distributions incorporating solar metal abundances provide an adequate and reasonable compromise.

The results of our fits to the combined Strömgren and low-dispersion IUE data are summarized in Figure 1. For PG 1104+243, the models are forced to match the observed  $u$  magnitude, rather than the  $y$  magnitude as is usually the case. This is because the  $b$  and  $y$  points are contaminated by the cool companion. A normalization at shorter wavelengths, near the long-wavelength end of the LWP camera, yields essentially the

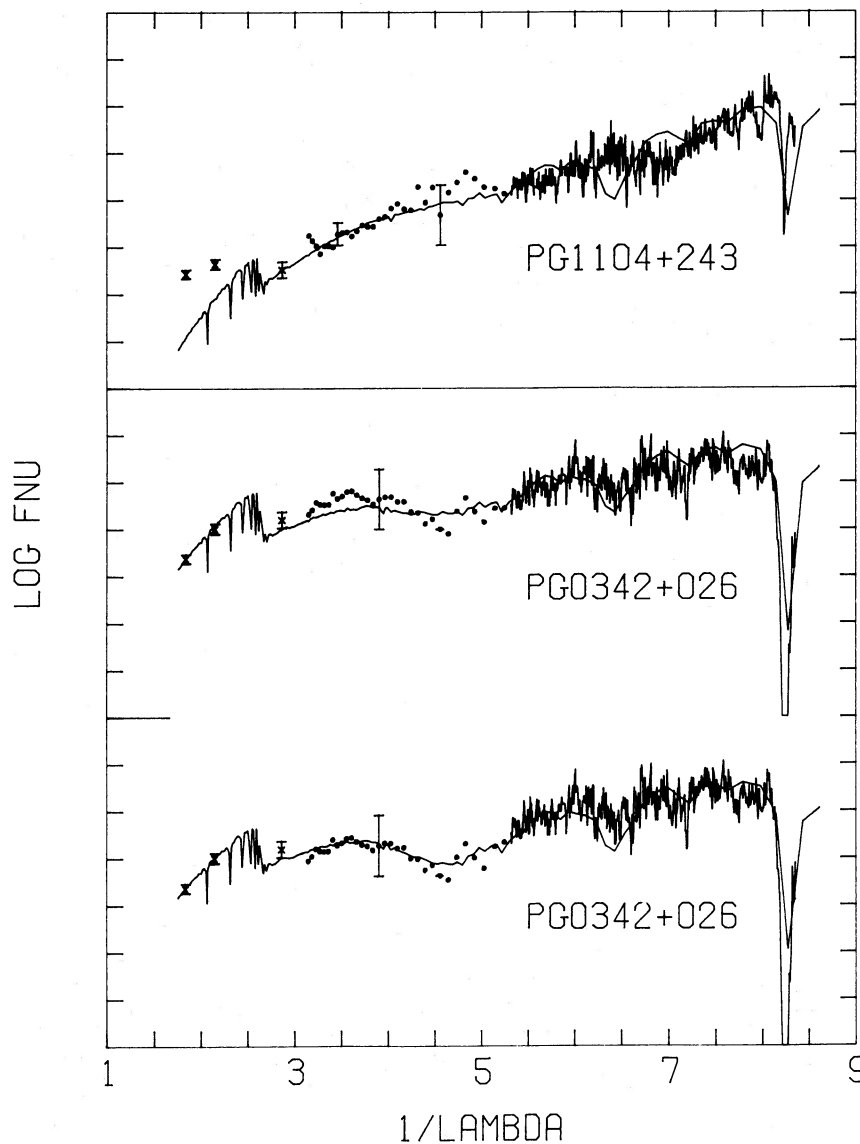


FIG. 1.—Energy distribution fits to our two stars. Strömgren  $u$ ,  $b$ , and  $y$  data, together with SWP (continuous line) and LWP (binned data) fluxes from the IUE ( $1/\lambda > 3 \mu\text{m}^{-1}$ ) are shown. Each tick mark represents 0.25 dex. Bars in the LWP region represent various estimates of the noise level in the data from that camera. Top panel, for PG 1104+243, displays an interpolated model at  $T_e = 27,200$  K,  $E(B-V) = 0.03$ . Bottom panel shows two fits to PG 0342+026. The first is the standard fit,  $T_e = 21,800$  K,  $E(B-V) = 0.06$ ; in the second, the LWP fluxes have been multiplied by a factor 0.9. The resulting fit is improved, at  $T_e = 23,200$  K,  $E(B-V) = 0.10$ .

same effective temperature for this object. We adopt thus  $T_e = 27,200 \pm 1500$  K,  $E(B-V) = 0.03$  for PG 1104+243.<sup>4</sup> Note that the predicted C IV  $\lambda 1550$  line in Kurucz's (1979) solar abundance models is stronger than is actually observed; the affected bins in the energy distribution fits were thus given zero weight.

Our fit to PG 0342+026 is also shown in the bottom panel of Figure 1. The top fit is our so-called standard fit, at  $T_e = 21,800 \pm 1500$  K,  $E(B-V) = 0.06$ . In the bottom fit we have multiplied the LWP fluxes by the empirical scaling factor (0.9) discussed in § II d. This is one case where the quality of the fit appears significantly improved, and the composite data now suggest  $T_e = 23,200$  K ( $E[B-V] = 0.10$ ). Since the latter value is based on rather crude arguments, this fit is presented here only as an indication of potential uncertainties associated with the LWP camera. The promised redetermination of the intensity transfer function of that camera (Imhoff 1984) may help remove some of the current worries associated with its use.

Once the effective temperature is determined, the surface gravity follows from a fit to the Balmer lines ( $H\beta$  and  $H\gamma$ ). The results for PG 0342+026 are shown in Figure 2; we determine  $\log g = 5.0 \pm 0.3$  for this object.<sup>5</sup> No such determination is possible for PG 1104+243, where the optical spectrum is obvi-

<sup>4</sup> The binary deconvolution method of Ferguson, Green, and Liebert (1984) yields a less accurate but consistent temperature for the primary of 28,000 K.

<sup>5</sup> The helium abundance in PG 0342+026 can also be inferred from our data. Our preliminary value,  $N(\text{He})/N(\text{H}) = 2 \times 10^{-3}$ , is consistent with other determinations in these helium-deficient objects (e.g., Heber *et al.* 1984b; Heber 1986).

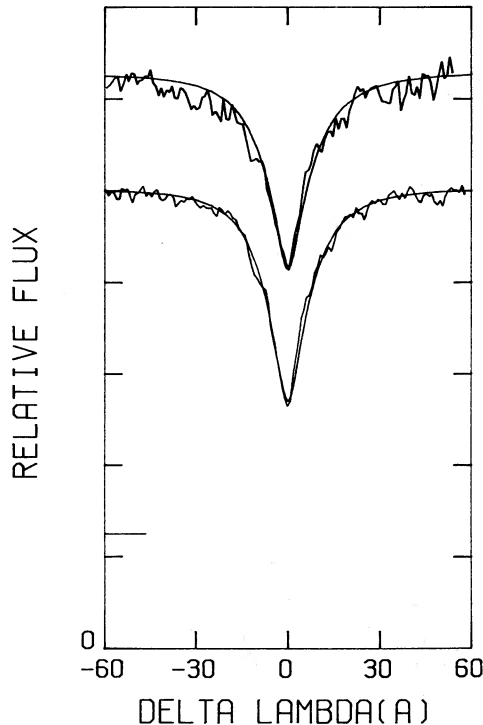


FIG. 2.—Fits to the  $H\beta$  (top) and  $H\gamma$  (bottom) profiles of PG 0342+026. Profiles shown are for  $T_e = 21,800$  K and  $\log g = 5.0$ . Both observed and theoretical profiles have been normalized at  $\pm 60$  Å from line center, and the theoretical profiles have been folded with a Gaussian of  $\text{FWHM} = 4.25$  Å. Zero point of lowermost plot is at bottom of figure; that of top plot is indicated by the long tick mark.

ously contaminated by the cool companion. In order to carry out our planned investigation of the metal abundance in that object, we have simply *adopted* a value of  $\log g = 5.5$  for PG 1104+243; this figure is the average surface gravity in the ensemble of 15 hydrogen-rich subdwarfs studied by Heber *et al.* (1984b) and Heber (1986). While this procedure may appear somewhat arbitrary, the distribution of surface gravity in that sample is relatively narrow ( $\sigma = 0.3$  dex). In the absence of any other gravity discriminant (e.g., a small-aperture Ly $\alpha$  profile from the IUE), our assumption appears quite reasonable.

#### b) Metal Abundance Analysis

The procedure followed to determine heavy-element abundances is identical to that used in our previous effort: model calculations are first performed at the values of  $T_e$  and  $\log g$  determined for each star (see § III a). These are LTE, hydrogen-line blanketed, metal-free models. Their principal utility is to provide a temperature stratification which is then used to compute detailed, synthetic spectra in the region of the metal lines of interest. In the latter part, metals are thus considered as trace elements—a reasonable assumption in view of the now well-documented underabundance of these ions in the photospheres of hydrogen-rich subdwarfs. For uniformity with our previous work, all abundances cited are obtained with the assumption of a microturbulent velocity of  $5 \text{ km s}^{-1}$  (see Paper I for further discussions of this point). Finally, the LTE line transfer used here is deemed perfectly adequate in view of the insignificance of non-LTE effects predicted in much hotter stars by BKSS.

#### IV. C, N, AND SI ABUNDANCES IN TWO STARS

The average element abundances obtained for the two stars under study are summarized in Table 3. They are generally based on the analysis of lines which originate on excited states, as indicated in Table 2. Resonance transitions, which are blended with their ISM counterparts, are used to check the self-consistency of the analysis. Let us now discuss briefly each element in turn.

##### a) Carbon

The carbon abundance relies on features of C II and C III. The C IV resonance doublet is quite strong, and the photospheric and interstellar components are blended in both objects; its analysis leads to upper limits on the C/H ratio consistent with the analysis of the higher excitation lines of C II and C III.

##### b) Nitrogen

This abundance determination relies on the analysis of N III features, principally the  $\lambda\lambda 1184$  and  $1759$  transitions. The resonance lines of N V are not seen in either object. N IV  $\lambda 1718.55$

TABLE 3  
SUMMARY OF ABUNDANCES

STAR	ABUNDANCES <sup>a</sup>		
	$\epsilon_C$	$\epsilon_N$	$\epsilon_{\text{Si}}$
PG 0342+026 .....	$7.0 \pm 0.6$	$8.6 \pm 0.8$	$5.6 \pm 0.7$
PG 1104+243 .....	$6.1 \pm 0.3$	$8.4 \pm 0.9$	$\leq 4$
Sun.....	8.5	8.0	7.5

<sup>a</sup>  $\epsilon_Z = 12 + \log [N(Z)/N(\text{H})]$ .

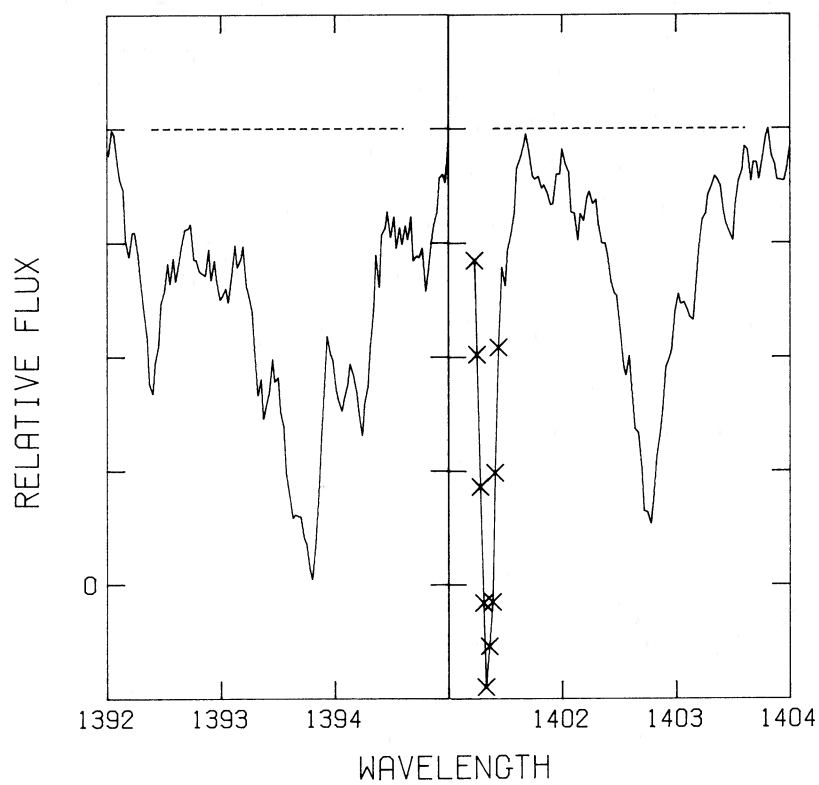


FIG. 3a

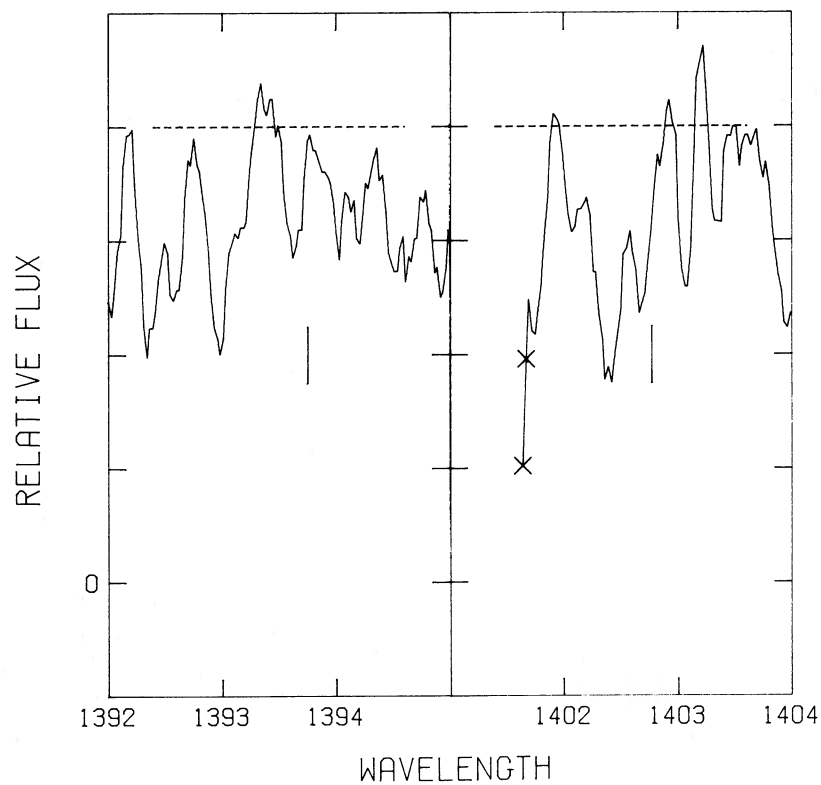


FIG. 3b

FIG. 3.—(a) Si IV  $\lambda\lambda$ 1393.76, 1402.77 region in PG 0342+026. Approximate continuum level is shown as a dashed line. Crosses indicate a reseau mark. (b) Same as (a) but for PG 1104+243. Long vertical marks indicate the expected location of the silicon features, based on the average radial velocity discussed in § IIc.

is seen, but some blending is undoubtedly present, especially in PG 1104+243. The only N II feature observable, N II  $\lambda$ 1886.82, could also be present in both stars.

### c) Silicon

This important element provides the largest spectroscopic contrast between our two objects. This is underscored by the appearance of the resonance lines of Si IV ( $\lambda\lambda$ 1393.76, 1402.77), shown in Figure 3a, b. This transition has been used in previous investigations (BKSS; BHS; Paper I) to set stringent upper limits to the silicon abundance in objects above 30,000 K. It is possible to show that this useful diagnosis tool can be extended to even lower temperatures. We display, in Figure 4, the variation of the total equivalent width of that transition as a function of  $T_e$  for various Si/H ratios. The model adopted here is one with  $\log g = 5.0$  and where the microturbulent velocity is fixed at  $\zeta = 5 \text{ km s}^{-1}$ . The line strength peaks at 30,000 K and remains a useful measure of the silicon abundance over essentially the whole temperature domain of the hydrogen-rich subdwarfs. In PG 1104+243, weak noise spikes were measured at  $-29$  and  $-19 \text{ km s}^{-1}$  and were used to obtain, single-handedly, the abundance limit given in Table 3. The latter is clearly a conservative upper limit. The usefulness of this Si IV transition for abundance determinations, even at lower values of  $T_e$ , eases considerably the burden of identifying the sometimes blended transitions of lower ionization states of Si (e.g., the Si III complex in the region 1294–1393 Å, with its N IV, S IV, and Ti III blends).

For PG 0342+026, the abundance value obtained from Si IV (which can be inferred from Fig. 4) has been averaged with those based on observed Si II and Si III lines to yield the average value given in Table 3.

## V. A REEXAMINATION OF METAL ABUNDANCE PATTERNS

With the two stars listed in Table 3, there are now nine hydrogen-rich subdwarfs for which high-dispersion IUE data has been collected and analyzed and C, N, and Si abundances

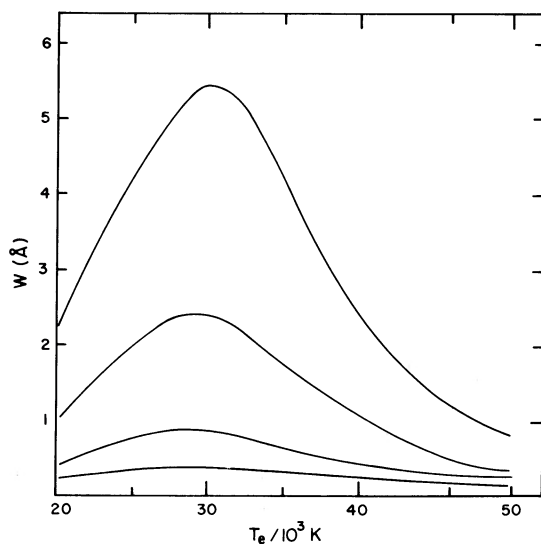


FIG. 4.—Total equivalent width (i.e.,  $W_{1393} + W_{1402}$ ) of the Si IV  $\lambda\lambda$ 1393.76, 1402.77 resonance transition in theoretical models at  $\log g = 5.0$  and with a microturbulent velocity  $\zeta = 5 \text{ km s}^{-1}$ . Curves are, from top to bottom, for  $\epsilon_{\text{Si}} = 8, 7, 6,$  and  $5$ .

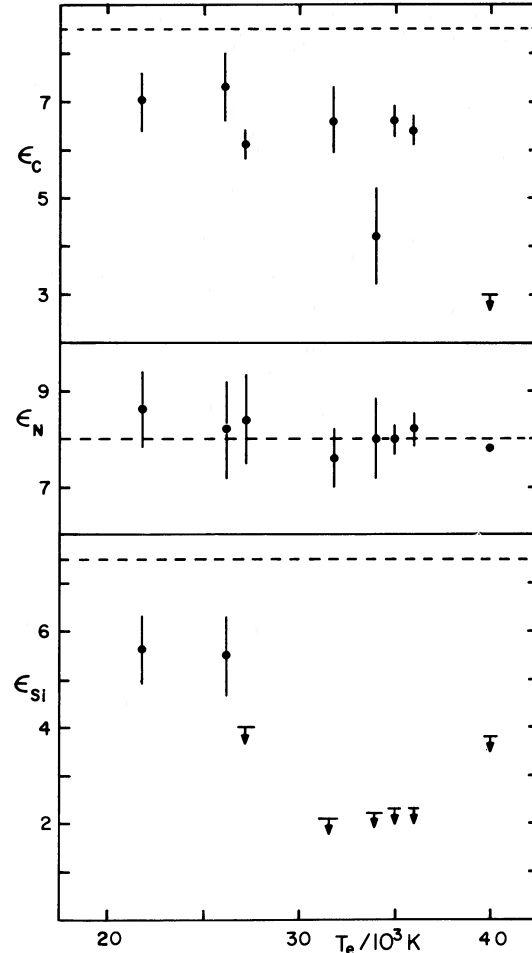


FIG. 5.—Summary of carbon, nitrogen, and silicon abundances determined up to now from high-dispersion IUE observations of hot, hydrogen-rich subdwarfs. In all three panels, the dashed line indicates the appropriate solar abundance. Individual effective temperatures are, in general, accurate to  $\sim \pm 1500\text{--}2000 \text{ K}$ .

derived. Hence a reexamination of the preliminary abundance patterns described in Paper I appears timely.

In Figure 5, the abundances determined for eight of these objects are shown as a function of the effective temperature. In contrast to Paper I, we have now left out LB 4539 from our discussion. This subdwarf, analyzed by Lynas-Gray *et al.* (1984), is in a close binary system ( $P = 6.3 \text{ hr}$ ). If the rotation period of the primary is synchronous with the orbital period, the surface velocity of the subdwarf would be of the order of  $40 \text{ km s}^{-1}$ . This is likely to have some influence on the diffusion processes under study; it thus seems appropriate to exclude LB 4539 from further discussion (a similar point is made by Vauclair and Liebert 1987). Also left out from Figure 5 are the results based on optical analyses obtained for two cool stars. This was done in order to provide a more homogeneous sample of objects, where abundances are all derived from model atmosphere analyses of high-dispersion ultraviolet data.<sup>6</sup>

<sup>6</sup> High-dispersion IUE images exist in the IUE merged log for both objects left out from Fig. 5, but included in Fig. 6 of Paper I. A progress report on the analysis of HD 205805 was published by Baschek, Kudritzki, and Scholz (1980). It seems likely that detailed analyses of that star and of HD 4539 will become available shortly.

Figure 5 shows that no surprises have emerged from our analysis, when our results are considered together with those of Paper I. The trend seen earlier in the carbon abundance is still present (i.e., a decreasing C/H ratio with increasing  $T_e$ ), although it now appears that the carbon abundance may perhaps not quite reach the solar value at low effective temperatures, as suspected earlier. The nitrogen abundance values determined here in PG 1104+243 and PG 0342+026 also confirm the result obtained earlier, i.e., a nearly solar abundance of N over the whole temperature domain. Lastly, the existence of that interesting silicon abundance pattern seems strengthened with our analysis: a comparison of the Si/H ratio in Feige 65 (Paper I)—at  $T_e = 26,200$  K—and in PG 1104+243 (this work)—at  $T_e = 27,200$  K—suggests that the observed drop in silicon abundance may well occur over a rather narrow temperature interval. Of some concern in this picture, however, is the near-normal silicon abundance observed in the cool sdB HD 205805 ( $T_e$  between 26,500 and 28,200 K); this result, obtained initially from optical studies by Baschek and Norris (1970), appears substantiated by the preliminary analysis of high-dispersion, ultraviolet spectra carried out by Baschek, Kudritzki, and Scholz (1980) and by our own inspection of these archival images. Of course, differences in surface gravity and uncertainties in the ascribed effective temperatures might play some role here as well. However, at this stage, the evidence for a sharp drop in the Si/H ratio offered in Figure 5 remains extremely suggestive. At low effective temperatures, we do not quite recover the solar silicon abundance, as originally suspected in Paper I. This behavior is similar to that encountered earlier with the C/H ratio. We suspect that a clearer picture of the abundances at low effective temperatures will become available with the analyses of additional cool sdB stars currently being performed by other groups (see note 6).

In a recent discussion, Michaud *et al.* (1985) have investigated the idea, put forth by BKSS, BHS, and Heber *et al.* (1984*a, b*), that the large Si underabundance observed in the

hotter objects could be due to a reduced radiative acceleration on that element, which is mainly in a rare gas configuration in the atmosphere. This explanation was shown to be incorrect, since the fraction of silicon not in the noble gas (Si v) configuration, although small, is always large enough in the atmosphere to guarantee the radiative support of more silicon than is actually observed. As an alternate picture, Michaud *et al.* suggested a slightly modified model, whereby diffusion processes would occur in the presence of a weak stellar wind. The interplay of these two competing particle transport processes then allows abundance peculiarities, similar to those observed, to develop over a time scale which depends critically on both the assumed mass-loss rate and the accuracy to which radiative forces can be calculated.

As part of our comprehensive investigation of hot, hydrogen-rich subdwarfs, we are currently reevaluating and improving upon previous calculations of radiative accelerations on metals in the atmospheres of these objects (Bergeron *et al.* 1987). While such theoretical work is indispensable for further progress in this area, it is clear that additional observations and abundance analyses, documenting the extent and the complexities of the abundance peculiarities observed in subdwarfs, are equally needed. The increasingly evident trends revealed in Figure 5 are a testimony to the success of this approach.

We are grateful to F. C. Bruhweiler for pertinent advice on high-dispersion observations, to F. Allard for her contribution to this analysis, and to the Astronomical Data Center at NASA/Goddard for providing archived images. We are, once again, indebted to the KPNO and IUE staff for their competent help in the acquisition and retrieval of our data, and to both facilities for the continued support of our observing program there. This work was supported in part by the NSERC Canada. Computing funds for this project were kindly made available by the Centre de Calcul of the Université de Montréal.

## REFERENCES

- Allard, F., Wesemael, F., Lamontagne, R., Fontaine, G., and Bergeron, P. 1987*a*, in preparation.  
 Allard, F., Wesemael, F., Lamontagne, R., Fontaine, G., and Bissonnette, Y. 1987*b*, in preparation.  
 Baschek, B., Höflich, P., and Scholz, M. 1982, *Astr. Ap.*, **112**, 76 (BHS).  
 Baschek, B., Kudritzki, R. P., and Scholz, M. 1980, in *Proc. 2d European IUE Conf.* (ESA SP-157), p. 319.  
 Baschek, B., Kudritzki, R. P., Scholz, M., and Simon, K. P. 1982, *Astr. Ap.*, **108**, 387 (BKSS).  
 Baschek, B., and Norris, J. 1970, *Ap. J. Suppl.*, **19**, 327.  
 Bergeron, P., Wesemael, F., Michaud, G., and Fontaine, G. 1987, in preparation.  
 Bohlin, R. C. 1986, *Ap. J.*, **308**, 1001.  
 Bohlin, R. C., and Holm, A. V. 1980, *NASA IUE Newsletter*, No. 10, p. 37.  
 Bruhweiler, F. C., and Kondo, Y. 1982, *Ap. J.*, **259**, 232.  
 Cassatella, A., and Harris, A. W. 1983, *NASA IUE Newsletter*, No. 23, p. 21.  
 Dean, C. A., and Bruhweiler, F. C. 1985, *Ap. J. Suppl.*, **57**, 133.  
 Ferguson, D. H., Green, R. F., and Liebert, J. 1986, *Ap. J.*, **287**, 320.  
 Fontaine, G., Wesemael, F., Lamontagne, R., Bergeron, P., and Green, R. F. 1987, in preparation.  
 Green, R. F., Schmidt, M., and Liebert, J. 1986, *Ap. J. Suppl.*, **61**, 305.  
 Greenstein, J. L., and Sargent, A. I. 1974, *Ap. J. Suppl.*, **28**, 157.  
 Hackney, R. L., Hackney, K. R. H., and Kondo, Y. 1982, in *Advances in Ultraviolet Astronomy: Four Years of IUE Research*, ed. Y. Kondo, J. M. Mead, and R. D. Chapman (Washington, DC: NASA), p. 335.  
 Heber, U. 1986, *Astr. Ap.*, **155**, 33.  
 Heber, U., Hamann, W.-R., Hunger, K., Kudritzki, R. P., Simon, K. P., and Mendez, R. H. 1984*a*, *Astr. Ap.*, **136**, 331.  
 Heber, U., Hunger, K., Jonas, G., and Kudritzki, R. P. 1984*b*, *Astr. Ap.*, **130**, 119.  
 Imhoff, C. L. 1983, *NASA IUE Newsletter*, No. 23, p. 20.  
 ———. 1984, *NASA IUE Newsletter*, No. 24, p. 21.  
 Kurucz, R. L. 1979, *Ap. J. Suppl.*, **40**, 1.  
 Lamontagne, R., Wesemael, F., Fontaine, G., and Sion, E. M. 1985, *Ap. J.*, **299**, 496 (Paper I).  
 Lynas-Gray, A. E., Heber, U., Kudritzki, R. P., and Simon, K. P. 1984, in *Proc. 4th European IUE Conf.* (ESA SP-218), p. 285.  
 Michaud, G., Bergeron, P., Wesemael, F., and Fontaine, G. 1985, *Ap. J.*, **299**, 741.  
 Oliverson, N. A. 1984, *NASA IUE Newsletter*, No. 24, p. 27.  
 Sonneborn, G. 1984, *NASA IUE Newsletter*, No. 24, p. 67.  
 Vauclair, G., and Liebert, J. 1987, in *Scientific Accomplishments of the IUE Satellite*, in press.  
 Wesemael, F., Holberg, J. B., Veilleux, S., Lamontagne, R., and Fontaine, G. 1985, *Ap. J.*, **298**, 859.

G. FONTAINE, R. LAMONTAGNE, and F. WESEMAEL: Département de Physique, Université de Montréal, C. P. 6128, Succ. A, Montréal, Québec PQ H3C 3J7, Canada